# Comparison between the Gamow shell model and cluster-orbital shell model for weakly bound systems

H. Masui*
*Information Processing Center, Kitami Institute of Technology, Kitami 090-8507, Japan*

K. Katō
*Department of Physics, Faculty of Science, Hokkaido University, Sapporo, 060-0810, Japan*

K. Ikeda
*The Institute of Physical and Chemical Research (RIKEN), Wako, 351-0198, Japan*
(Dated: May 11, 2007)

We study contributions of poles and continua of the single-particle states to the wave function obtained by the cluster-orbital shell model (COSM). The COSM wave function is described in terms of a linear combination of non-orthogonal Gaussian basis sets. We study oxygen and helium isotopes as examples of normal and weakly bound nuclei. In the investigation of the contribution of the single-particle states, we expand the COSM wave function by using an extended completeness relation, which is constructed by the solution of the single-particle Hamiltonian. We use the complex scaling method to obtain the bound, resonant and continuum states of the Hamiltonian and construct the extended completeness relation. The results are compared with those obtained by the Gamow shell model calculation.

PACS numbers: 21.10.-k, 21.60.-n

## I. INTRODUCTION

The field of nuclear physics has been extended toward the drip-lines of the neutron and proton [1–8]. In the drip-line regions, it has been revealed that we cannot directly apply our knowledge on the stable nuclei, since the basic understandings such as the saturation property and the magic-number observed in the stable nuclei seems to be inapplicable for describing the properties of drip-line nuclei. Further, different from the drip-line nuclei from stable nuclei, the role of unbound states becomes very important. Because weakly bound nuclei have few bound states and other excited states are unbound states. Coupling to the unbound states should be taken into account to describe the systems. In order to understand new phenomena and properties of such the drip-line nuclei, it is necessary to develop a new approach, which is suitable and has an ability to treat the typical features of these nuclei.

In the ground and low-lying excited states, a mean-field description has been employed as a zeroth order approximation to treat nuclear many-body correlations [9–12]. Recent years, in the mean-field approach, an explicit treatment of bound-continuum and continuum-continuum couplings has been developed. The Gamow shell model [13–19] is one of the most successful approaches to treat the coupling to the continuum. In GSM, the completeness relation is defined by using the Berggren metric [20, 21] on the complex momentum plane with the bound, resonant, and continuum states. The two-body matrix elements of GSM involving the Gamow states [22] can be calculated with a careful treatment of the integration path of the coordinates.

At the beginning of unstable nuclear physics, a surprising evidence of the two-neutron halo was discovered in $^{11}$Li [23]. It has been pointed out that a di-neutron like correlation plays an important role in order to understand the exotic property of the neutron halo [24–26]. A direct way to treat the nucleon-nucleon correlation is considered to be a few-body approach based on the frame work including rearrangement channels of different coordinate systems of the core+$n$+$n$ model space. For light drip-line nuclei, such as $^{6}$He and $^{11}$Li, the so called "hybrid-TV model" has been developed and successfully describes the two-neutron halo structure of those nuclei [25–27]. The hybrid-TV model is a combination of the cluster-orbital shell model (COSM), which is suitable to describe the mean-field correlation of the valence nucleons, and the extended cluster model (ECM), in which the di-neutron correlation can be fully described with an appropriate boundary condition. Form the intuitive picture of the coordinate systems of COSM and ECM, the basis sets are called V- and T-bases, respectively. Using the hybrid-TV model, the precise investigations of the halo structure have been done through the study of bound and resonant states and the break up reactions [25–28].

However, as the number of valence nucleon increases, i.e. more than two nucleons, it becomes difficult to directly apply the hybrid-TV model for solving systems with many valence nucleons. Therefore, it is necessary to investigate applicability of COSM to such the many-valence-nucleon systems. Further, it is worthwhile to see ability for describing nucleon-nucleon correlations especially the components of the di-neutron correlation.

*Electronic address: hgmasui@mail.kitami-it.ac.jp

Recently, we proposed an extended cluster-orbital shell model approach [29]. In Ref.[29], we performed a stochastic variational calculation to solve the motion of the valence nucleons around the core.

In this work, we study oxygen and helium isotopes with the COSM formalism in a core+$XN$ model space and investigate the contributions of poles and continua to the wave function obtained by COSM. To study the contribution of the poles and continua, we use an extended completeness relation obtained by applying the complex scaling method to the single-particle Hamiltonian. We expand the wave function of COSM by using the extended completeness relation and perform a comparison between the COSM and GSM approaches.

In the section 2, we briefly show a formalism of COSM. Also, definition of the completeness relation by using CSM is given. In section 3, calculated results for oxygen and helium isotopes are shown, and we compare our COSM results to GSM. Summary and discussion are given in section 4.

## II. FORMALISM OF THE CLUSTER-ORBITAL SHELL MODEL

### A. Cluster orbital shell model

We briefly explain the formalism of COSM [30]. In COSM, the Hamiltonian of the total system, from which the center of mass motion $\hat{T}_G$ is subtracted, is described by the core and valence parts as follows:

$$\begin{aligned}\hat{H} &= \sum_{i=1}^{A}\hat{t}_i - \hat{T}_G + \sum_{i<j}^{A}\hat{v}_{ij} \\ &= \hat{H}_C + \sum_{i\in V}(\hat{t}'_i + \hat{V}'_i) + \sum_{i<j\in V}(\hat{T}_{ij} + \hat{v}_{ij}) \\ &= \hat{H}_C + \sum_{i\in V}\hat{h}_i + \sum_{i<j\in V}\hat{O}_{ij}\ . \end{aligned} \tag{1}$$

Here, $A$ is the mass number of the total system and "V" in the sum represents valence nucleons. $\hat{H}_C$ is the Hamiltonian for nucleons in the core. $\hat{T}_{ij}$ is the two-body kinetic operator of the form $\hat{T}_{ij} = \frac{1}{\mu}\nabla_i \cdot \nabla_j$, which comes from the subtraction of the center of mass motion in the COSM coordinate system spanned from the center of mass of the core to each valence nucleon. See Fig. 1. $\hat{t}_i$ and $\hat{t}'_i$ are one-body kinetic operators, and $\hat{t}'_i$ is defined by the relative motion between the core and the $i$th valence nucleon. The one-body potential for the $i$th valence nucleon is defined by taking the sum for the nucleons in the core: $\hat{V}'_i = \sum_{k\in C}\hat{v}_{ik}$. As shown in Eq.(1) the total Hamiltonian is described by the core part; $\hat{H}_C$, and one-body part; $\hat{h}_i \equiv \hat{t}'_i + \hat{V}'_i$, which corresponds to the one-body Hamiltonian between the core and a valence nucleon, and two-body part; $\hat{O}_{ij} \equiv \hat{T}_{ij} + \hat{v}_{ij}$.

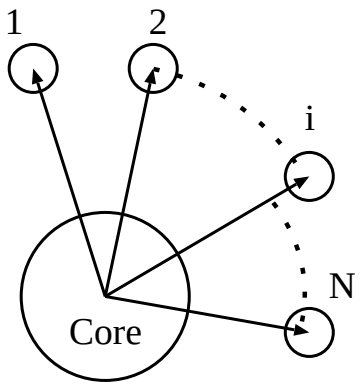


FIG. 1: Coordinate system of the cluster-orbital shell model spanned from the center of mass of the core to each valence nucleon.

We define the wave function $|\Psi\rangle$ by taking anti-symmetrization between nucleons in the core and valence parts, $|\Phi_C\rangle$ and valence $|\Phi_V\rangle$ as follows:

$$|\Psi\rangle \ = \ \mathcal{A}'\Big\{\ |\Phi_C\rangle\,|\Phi_V\rangle\Big\}\ . \tag{2}$$

Here $|\Phi_C\rangle$ and $|\Phi_V\rangle$ are individually anti-symmetrized, and $\mathcal{A}'$ stands for the anti-symmetrization between nucleons in $|\Phi_C\rangle$ and $|\Phi_V\rangle$. In our COSM formalism, the valence part is described by a linear combination of the Gaussian with different width parameters as follows:

$$\begin{aligned}\Phi_V &= \sum_m c^{(m)}\Phi^{(m)}_{JM} \\ &= \sum_m c^{(m)}\mathcal{A}\Big\{F^{(m)}(r_1,\cdots,r_N)\cdot|JMTM_T{}^{(m)}\rangle\Big\}\ .\end{aligned} \tag{3}$$

Here, the radial part $F^{(m)}(r_1, r_2, \cdots)$ is the products of the Gaussian functions as follows:

$$F^{(m)}(r_1,\cdots,r_N) \equiv g_1^{(m)}(r_1)\cdots g_N^{(m)}(r_N)\ . \tag{4}$$

The Gaussian radial function is defined by the width parameter $a$ with an normalization $\mathcal{N}$ as $g(r) = \mathcal{N}r^l\exp(-\frac{a}{2}r^2)$. The angular momentum part is constructed by the normal coupling scheme:

$$\begin{aligned}&|JMTM_T{}^{(m)}\rangle \\ &= [[[j_1^{(m)}, j_2^{(m)}]_{J_{12}}, j_3^{(m)}]_{J_{123}}, \cdots]_{JM}\cdot\chi(T\,M_T)\ .\end{aligned} \tag{5}$$

where, $\chi(T\,M_T)$ is the total isospin function. In the case that all the valence nucleons are the same, i.e. all valence particles are neutrons or protons, we do not calculate the isospin part explicitly.

In a two-valence-nucleon case, we can perform a calculation using a sufficiently large number of basis sets. This corresponds to a microscopic three-body calculation in a core+$N$+$N$ model space with the "V" coordinate system. For three- or more-valence-nucleon cases, it is necessary to reduce the number of basis sets by using an efficient way. In our COSM calculation, widths $a_i^{(m)}$ of the

Gaussian and angular momenta in $j_i^{(m)} = ([l_i \otimes s_i]_{j_i})^{(m)}$ are considered to be the parameters of the calculation. The parameter sets are chosen using a sort of the stochastic variational technique, in order to reduce the number of basis sets. Using the stochastically chosen basis sets, we diagonalize the Hamiltonian of the core part and obtain the eigen function $|\Phi_V\rangle$ as a linear combination of the basis sets $\Phi_{JM}^{(m)}$ with different width parameters $a_i^{(m)}$ and angular momenta $j_i^{(m)}$.

The expression of the wave function using a linear combination of the products of the Gaussian functions is widely applied in few-body calculations. Hence, in the viewpoint of the asymptotic condition, the linear combination of $F^{(m)}(r_1, r_2, \cdots)$ has the correct $N$-body bound state boundary condition. For the resonant states in two valence nucleons cases, we can obtain the correct resonant states by applying the complex scaling method.

### B. Completeness relations obtained by different methods

In our COSM approach, the wave function is a linear combination of the products of the non-orthogonal functions of each core-$N$ sub-system. On the other hand, in GSM, the basis sets are constructed from the core-$N$ eigen states, and the completeness relation is applied to include the continuum contribution to the wave function.

Therefore, in order to compare our approach to GSM, it is necessary to prepare the complete set of the core-$N$ eigen states, and to expand the total wave function using the complete sets.

In the normal case that the contour of the momentum is taken on the real axis, the completeness relation for the $i$th valence nucleon is defined as follows:

$$\mathbf{1}_i = \sum_{n=b} |\phi_i^{(n)}\rangle\langle\tilde{\phi}_i^{(n)}| + \oint_L dk\, |\phi_i(k)\rangle\langle\tilde{\phi}_i(k)| \ , \qquad (6)$$

where "$b$" in the sum stands for bound states. With this definition, only the bound states are inside the closed path of the integration, that is shown in Fig. 2(a). In the GSM calculations, the contour path of the momentum is deformed so that the resonant poles are included in the closed path, as shown in Fig.2(b). In this case, the completeness relation is defined by the bound and resonant states and the continuum with deformed contour path $L'$ as follows:

$$\mathbf{1}_i = \sum_{n=b,r} |\phi_i^{(n)}\rangle\langle\tilde{\phi}_i^{(n)}| + \oint_{L'} dk\, |\phi_i(k)\rangle\langle\tilde{\phi}_i(k)| \ , \qquad (7)$$

where "$r$" in the sum stands for resonant states. The path in Fig. 2(b) is one of the example. The contour path on the real momentum axis is deformed so that two resonant poles are included in the closed path. In practice, the contour path is discretized and the integration for $L'$ is done by taking the sum of the discretized complex momentum.

$$\oint_{L'} dk\, |\phi_i(k)\rangle\langle\tilde{\phi}_i(k)| = \sum_n w_{(n)} |\phi_i(k^{(n)})\rangle\langle\tilde{\phi}_i(k^{(n)})| \ . \qquad (8)$$

Here, the weight $w_{(m)}$ should be determined for the discretized continuum states, appropriately.

In the case that the system has a many-particle resonant state, the contour path should be chosen carefully. The poles of the many-particle resonant state are not necessarily enclosed with the contour paths of the single-particle states, because the position of the many-particle resonant poles are determined after solving the eigen value problem of the system using the single particle states.

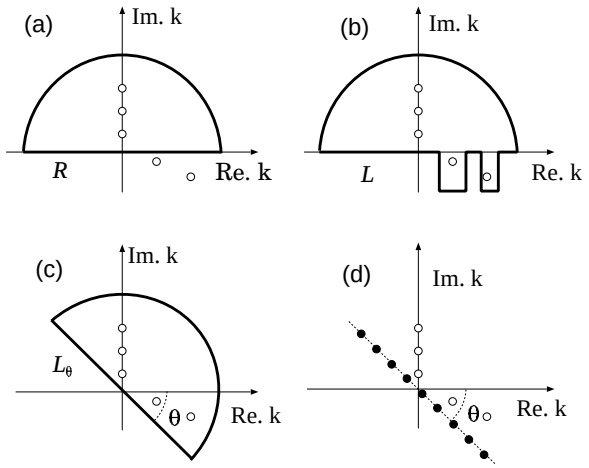


FIG. 2: Definition of contour on the complex momentum plane and location of the poles and continua.

We employ an efficient way to define the complete set, that is the complex scaling method (CSM) [31–34]. In CSM, the coordinate (momentum) is rotated as $r \to re^{i\theta}$ ($p \to pe^{-i\theta}$) in the complex coordinate (momentum) plane. The resonant states become the $L^2$-integrable that the wave functions have the same boundary condition of the bound states. It is shown as the so-called "ABC-theorem" [31, 32]. The integration of the closed path of the momentum is carried out along a rotated semi-circle on the complex momentum plane as shown in Fig. 2(c). The resonant poles are enclosed by the rotated semi-circle on the diameter $L_\theta$, and continuum states on the real axis are on the rotated line for the rotation angle $\theta$. Using the complex-scaled eigen vectors $\phi_\theta^{(m)}$, we obtain the extended completeness relation [34] as follows:

$$\mathbf{1}_i = \sum_{n=b,r} |\phi_{\theta,i}^{(n)}\rangle\langle\tilde{\phi}_{\theta,i}^{(n)}| + \oint_{L_\theta} dk\, |\phi_{\theta,i}(k)\rangle\langle\tilde{\phi}_{\theta,i}(k)| \ . \qquad (9)$$

In the actual CSM calculation, the eigen states are obtained by using a matrix diagonalization of the complex-scaled Hamiltonian with a complex-scaled finite basis set:

$H_\theta|\phi_\theta\rangle = E|\phi_\theta\rangle$. Each eigen state is constructed by a linear combination of the basis functions, e.g. Gaussian. Due to the finiteness of the basis set, the continuum states are obtained as the eigen vectors with discrete complex energies along the $2\theta$-line on the complex energy plane. A schematic figure on the complex momentum plane, where $E = k^2/2\mu$ and continua are on the $\theta$-line, is shown in Fig. 2(d). Hence, all states are obtained as a discrete set of eigen vectors as:

$$\oint_{L_\theta} dk|\phi_{\theta,i}(k)\rangle\langle\tilde{\phi}_{\theta,i}(k)| = \sum_n |\phi_{\theta,i}(k_\theta^{(n)})\rangle\langle\tilde{\phi}_{\theta,i}(k_\theta^{(n)})|, \quad (10)$$

It has been shown that the discretized continuum states fulfill the extended completeness relation with the bound and resonant states obtained by CSM [34]. Moreover, we do not need to determine the weight of each eigen state as done in the GSM case for the construction of the completeness relation. The weight is automatically determined and included in the complex normalization of the eigen state though the matrix diagonalization.

Using CSM for resonant states and discretized continuum states, we obtain the extended completeness relation for the $i$the particle as follows:

$$\begin{aligned} \mathbf{1}_i &= \sum_{m=b,r} |\phi^{(m)}_{\theta,\,i}\rangle\langle\tilde{\phi}^{(m)}_{\theta,\,i}| + \oint_{L_\theta} dk\,|\phi_{\theta,\,i}(k)\rangle\langle\tilde{\phi}_{\theta,\,i}(k)| \\ &\equiv \sum_\nu |\phi_{\theta,\,i}[\nu]\rangle\langle\tilde{\phi}_{\theta,\,i}[\nu]| \ . \end{aligned} \quad (11)$$

Here, $|\phi_\theta[\nu]\rangle$ are $|\phi^{(\nu)}_\theta\rangle$ for bound and resonant states (pole states) and $|\phi_\theta(k^{(\nu)}_\theta)\rangle$ for the discretized continuum states. $\nu$ is the label of the eigen states representing the bound, resonant and discretized continuum states.

### C. Relation between COSM and GSM

In order to investigate the relation between COSM and GSM, we expand the wave function obtained by COSM in terms of the core-$N$ eigen functions $\{\phi_\theta[\nu_i]\}$ using the extended completeness relation (11) as

$$\begin{aligned} |\Psi_V\rangle &= \mathbf{1}_1 \otimes \cdots \otimes \mathbf{1}_N \sum_m c^{(m)} \mathcal{A}\left\{ F^{(m)}\,|JMTM_T{}^{(m)}\rangle \right\} \\ &= C_1\,|(\phi_{\theta,\,1}[\nu_1]\cdots\phi_{\theta,\,N}[\nu_N])_1\rangle \\ &\quad + C_2\,|(\phi_{\theta,\,1}[\nu'_1]\cdots\phi_{\theta,\,N}[\nu'_N])_2\rangle + \cdots \\ &= \sum_k C_k\,|(\phi_{\theta,\,1}[\nu_1]\cdots\phi_{\theta,\,N}[\nu_N])_k\rangle \ . \end{aligned} \quad (12)$$

Here, $(\phi\,\phi\cdots)_k$ stands for a set of the component of the core-$N$ eigen vectors with a combination of angular momenta and corresponds to the GSM basis. $C_k$ is a coefficient of the expansion defined by the overlap between single-particle states and the COSM wave function as follows:

$$C_k \equiv \langle(\tilde{\phi}_{\theta,1}[\nu_1]\cdots\tilde{\phi}_{\theta,N}[\nu_N])_k|\Psi_V\rangle, \quad (13)$$

where the suffix $k$ in $C_k$ is a label of the set of eigen states; $k\{\nu_1,\nu_2,\cdots,\nu_N\}$. The coefficient $C_k$ in Eq. (13) corresponds to the weight of the basis set in GSM.

In practice, the radial part of the eigen function of each single-particle state $\phi_\theta$ is also represented as a linear combination of the Gaussian,

$$\begin{aligned} \phi_\theta(r) &= \sum_{m'} d^{(m')}\,u^{(m')}(re^{i\theta}) \\ &= \sum_{m'} d^{(m')}\,g^{(m')}(re^{i\theta})\cdot\{[l\otimes s]_j\cdot\chi^\tau\}^{(m')} \end{aligned} \quad (14)$$

Therefore, the coefficient $C_k$ can be calculated easily and be performed in analytically.

## III. APPLICATION OF COSM TO OXYGEN AND HELIUM ISOTOPES

### A. Energies and r.m.s.radii of oxygen and helium isotopes

We study oxygen and helium isotopes by COSM as examples for the stable and weakly bound nuclei respectively. The basis sets are selected by using a stochastic method, which is performed in Ref.[29]. We show calculated energies, levels and r.m.s.radii for these nuclei.

#### *1. Oxygen isotopes*

First, we show the calculated energies, levels and r.m.s.radii for oxygen isotopes as an example of stable nuclei. This calculation is the same one performed in Ref.[29]. The size parameter of the core is fixed in this calculation.

We construct the interaction between the core and a valence nucleon (the core-$N$ interaction) microscopically by folding a nucleon-nucleon interaction with the core wave function as follows:

$$\hat{V}'_i|\Phi_V\rangle \equiv \sum_{k\in C}\left\langle\Phi_C\ \middle|\ \hat{v}_{i\,k}\ \middle|\ \mathcal{A}\left\{\ |\Phi_C\rangle\,|\Phi_V\rangle\right\}\right\rangle \simeq \hat{V}^d_i + \hat{V}^{ex}_i \ . \quad (15)$$

Here, $\hat{V}^d_i$ and $\hat{V}^{ex}_i$ are the direct and exchange parts, respectively. The exchange part is only considered "knock-on" exchange term described in Ref.[35]. we assume the lowest configuration of the harmonic oscillator wave function of $^{16}$O and use the core-size parameter $b_C = 1.723$ (fm) so as to reproduce the r.m.s.radius of $^{16}$O within the experimental error bars.

The Pauli principle between nucleons in the core and a valence one is treated in terms of the orthogonality condition model (OCM) [36]. As an conventional method to

eliminate the forbidden states, we use a pseudo potential $\lambda\hat{\Lambda}_i = \lambda|F.S.\rangle\langle F.S.|$, where $|F.S\rangle$ stands for the Pauli forbidden states. As taking $\lambda \to \infty$ in the calculation, the forbidden states are effectively eliminated.

Additionally, we introduce an effective $LS$ potential $\hat{V}_i^{ls}$ to reproduce the energy splitting of the low-lying positive parity states $5/2^+$ and $3/2^+$ of $^{17}$O.

The Hamiltonian of the core-$N$ part for the $i$th valence nucleon $\hat{h}_i$ becomes as follows:

$$\hat{h}_i = \hat{t}'_i + \hat{V}_i^d + \hat{V}_i^{ex} + \hat{V}_i^{ls} + \lambda\hat{\Lambda}_i \ . \tag{16}$$

For the two-body interaction $\hat{v}_{ik}$, we use the Volkov No.2 interaction [37]. The parameters of the interaction is determined so that the energies of the lowest three positive parity states of $^{17}$O; $5/2^+$, $1/2^+$ and $3/2^+$, and the gourd state of $^{18}$O are reproduced. For details, see Ref.[29].

Calculated one-neutron separation energies ($S_n$) and r.m.s. radii ($R_{rms}$) are shown in Table I. Since we calculated the binding energies defined by the $^{16}$O+$Xn$ threshold, the separation energy is deduced by using the following definition:

$$S_n(A) = E(A-1) - E(A) \ . \tag{17}$$

Both $S_n$ and $R_n$ are in a good agreement with the observed values. This result shows that our COSM can reasonably describe the ground state properties.

| | $^{17}$O | $^{18}$O | $^{19}$O | $^{20}$O |
|---|---|---|---|---|
| $S_n$ (MeV) | | | | |
| Calc. | 4.143 | 8.048 | 4.204 | 7.331 |
| Exp. [38, 39] | 4.143 | 8.044 | 3.957 | 7.607 |
| $R_{rms}$ (fm) | | | | |
| Calc. | 2.59 | 2.64 | 2.67 | 2.71 |
| Exp. [1] | $2.59 \pm 0.05$ | $2.61 \pm 0.08$ | $2.68 \pm 0.03$ | $2.69 \pm 0.03$ |

TABLE I: Calculated $S_n$ and $R_{rms}$ of oxygen isotopes and experimental data.

We also calculate the energy levels of the oxygen-isotopes. Results are shown in Figs.3 to 5. The GSM calculations are taken form Ref.[14]. In $^{18}$O, we perform the same calculation in Ref.[29], where the basis sets are prepared in sufficiently large number and the stochastic approach is not used in the calculation. Hence, excited states with the same spin parity of the lowest states including resonant states can be calculated by applying CSM.

In $^{19}$O and $^{20}$O, we perform the stochastic approach to chose the basis set. Therefore, we can only obtain the lowest states for each spin parity. And, for $^{20}$O, we only perform the calculation for $0^+$ and $2^+$. As seen in Figs.3 to 5, our calculation shows a good agreement to the experiments.

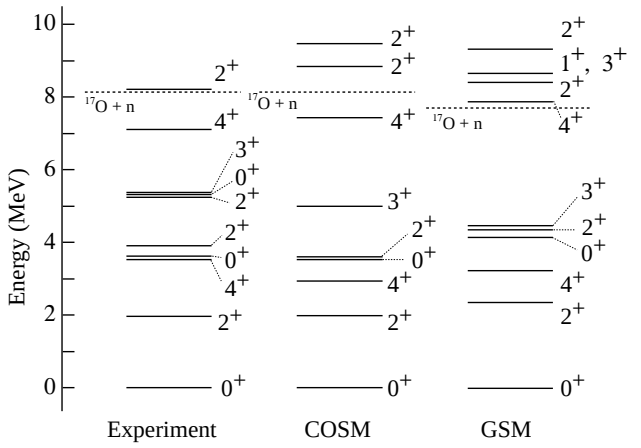


FIG. 3: Calculated energy levels of $^{18}$O. Experimental data are taken from Ref.[39]. The GSM results are taken from Ref.[14]. See text.

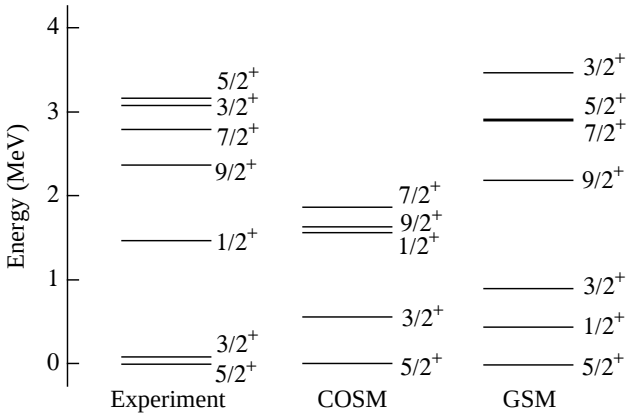


FIG. 4: Calculated energy levels of $^{19}$O. Experimental data are taken from Ref.[39]. The GSM results are taken from Ref.[14]. See text.

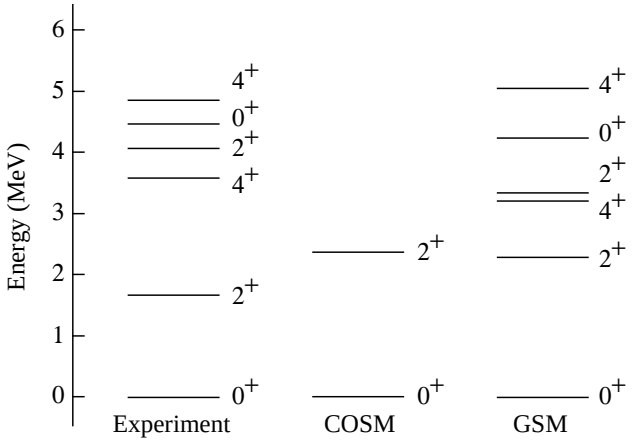


FIG. 5: Calculated energy levels of $^{20}$O. Experimental data are taken from Ref.[39]. The GSM results are taken from Ref.[14]. See text.

### 2. Helium isotopes

Next, we show calculated energies and r.m.s.radii for helium isotopes as an example of weakly bound nuclei.

Helium isotopes have been studied in $^4$He+$Xn$ model, since the $^4$He-core is a strongly bound system and the excitation energy to the first excited state is very large. In this calculation the $^4$He-core is considered to be inert and has the $(0s)^4$ configuration.

We use the so called "KKNN"-potential [40] as the interaction between the $^4$He core and a valence nucleon. The KKNN-potential was constructed from a treatment based on the RGM approach with $(0s)^4$-core to reproduce the phase shifts of the $^4$He+$n$ scattering. The local potential form is the direct part $\hat{V}_i^d$ and $LS$ part $\hat{V}_i^{ls}$. We use OCM to treat the Pauli principle in the core nucleons, same as the oxygen isotope case. Hence, the single-particle Hamiltonian for $i$th valence nucleon becomes as follows:

$$\hat{h}_i = \hat{t}_i' + \hat{V}_i^d + \hat{V}_i^{ls} + \lambda\hat{\Lambda}_i \ . \tag{18}$$

We solve the complex scaled Hamiltonian $\hat{h}_i(\theta)$ of $^5$He using CSM and obtain the low-lying resonant states of $3/2^-$ and $1/2^-$ as $0.74 - i0.29$ (MeV) and $2.11 - i2.94$ (MeV), respectively. Using the KKNN-potential, the resonant poles of $^5$He of lowest two states ($3/2^-$ and $1/2^-$) are well reproduced.

For valence nucleons, we use the same interactions used in the precise three-body model calculations of $^6$He [25, 27]. The Minnesota effective potential [41] with the exchange parameter $u = 1.0$ is used for the two-body interaction, and an effective three-body interaction between the $^4$He and two valence nucleons is employed [27], which is introduced to simulate the effect of the excitation of the core and to fit the binding energy of $^6$He.

We calculate the ground state energies and r.m.s.radii of the helium isotopes. Calculated energies from the $^4$He+$Xn$ threshold are shown in Table II. Due to the lack of the model space in COSM, where the rearrangement coordinate system is not introduced, the energy of $0^+$ ground state of $^6$He is obtained as $-0.79$ (MeV), while the experimentally observed one is $-0.98$ (MeV). Nevertheless, the calculated energies almost agree with the experimental data within $\sim 0.3$ (MeV) of the average deviation.

| | | $^5$He | $^6$He | $^7$He | $^8$He |
|---|---|---|---|---|---|
| E. (MeV) | GSM [14] | 0.75 | −0.98 | 0.18 | −1.60 |
| | GSM [19] | 0.75 | −0.98 | −0.14 | — |
| | COSM | 0.74 | −0.79 | −0.89 | −2.94 |
| | Exp. [42] | 0.89 | −0.98 | −0.53 | −3.11 |

TABLE II: Calculated energies of Helium isotopes and experimental data [42]. Values of the GSM calculations in the second line are taken from Fig. 19 in Ref. [14].

The calculated r.m.s.radii of the helium isotopes are shown in Table III. There are several experimental observations which show different radii for $^6$He and $^8$He due to the difference of the analysis [43–45]. From the intuitive understanding of the isotopes, $R_{rms}$ become larger as the number of valence neutrons grows. Especially, in weak-binding systems, the radii of nuclei grow very rapidly, due to the broad tail of the valence neutrons. The COSM calculation shows qualitative agreement to the experiments of Ref. [44] and Ref. [45]. Quantitatively, we obtain the good agreement for $^6$He to the experiment Ref. [43], but at the same time the $^8$He radius of our calculation becomes much larger than the experiment [43].

| | Calc. | Exp.: Ref.[43] | Ref.[44] | Ref.[45] |
|---|---|---|---|---|
| $^6$He | 2.48 | $2.48 \pm 0.03$ | $2.33 \pm 0.04$ | $2.30 \pm 0.07$ |
| $^8$He | 2.66 | $2.52 \pm 0.03$ | $2.49 \pm 0.04$ | $2.45 \pm 0.07$ |

TABLE III: Matter r.m.s. radii of helium isotopes. All units are fm.

However, it should be noted that mean-field like coordinate systems, which are defined from the center of mass of the core or a definite origin of the total system to each valence nucleon, can not fully describe the nucleon-nucleon correlation among the valence nucleons. As pointed out in the works on $^6$He [25], the COSM coordinate system needs higher-orbital angular momenta ($l \leq 15$) to reproduce the $0^+$ ground state of $^6$He. An alter coordinate system is necessary to be introduced to compensate for the lack of the model space. In $^6$He, the "T"-type coordinate system, which is called as the extended cluster model [25], is very important to take into account the correlation of the valence nucleon and reproduce the binding energy. Otherwise, if we try to describe the system in the COSM model space, we need to modify the interaction between valence nucleons in order to take account the effect of the nucleon-nucleon correlation.

## B. Poles and continua contributions: comparison between COSM and GSM

Our COSM calculation for the oxygen and helium isotopes shows a good agreement to the experiments about energies and r.m.s.radii. Recently, weakly bound nuclei such as helium isotopes are studied in the GSM approaches [14, 19]. As shown in Sec. 2, COSM and GSM are related by the coefficients of the basis function $c^{(m)}$ and $C_k$ in Eqs. (3) and (12). The essential difference between COSM and GSM is the treatment of the unbound components of the single-particle states. Our COSM approach describes the components of unbound states as the linear combination of the Gaussian basis sets. Each basis set has convergent asymptotic behavior and is not an eigen state of the single-particle Hamiltonian. Hence, the components of unbound states in the wave function are treated implicitly. In GSM, on the other hand, the components of the unbound states are included to the wave function in terms of the explicit treatment of the

continuum states for the basis sets. Therefore, it is worth to investigate the correspondence between COSM and GSM.

### 1. Oxygen isotopes

In order to prepare the complete set of the $^{16}$O+$n$ subsystem, we solve the complex-scaled Hamiltonian of the $^{17}$O system and construct the extended completeness relation using the eigen functions. In this calculation, the rotation angle of the complex scaling is taken as $\theta = 10$ (degree). With this rotation angle, only one resonant state of $3/2^+$ $(0d_{3/2})$ is obtained. Resonant states of other higher angular momentum states have large decay width and cannot be obtained with this rotation angle.

As an example, in the case of the $0^+$ ground state of $^{18}$O, the wave function can be expanded in terms of the core+$n$ eigen functions according to Eq. (12) as follows:

$$|\Psi_V(0^+)\rangle = \mathbf{1}_1 \otimes \mathbf{1}_2 |\Psi_V(0^+)\rangle \quad (19)$$

$$= C_1 \,|(\phi_{0d_{5/2}})^2\rangle + C_2 \,|(\phi_{1s_{1/2}})^2\rangle + \cdots \ .$$

Here, $\phi_{lj}$ are single-particle eigen states, and the definition of $C_k$ is the same as Eq. (13).

The weights $C_k$ are classified by the number of poles and continua in the basis function. In $^{18}$O, the combination of the core-$N$ components are three kinds; (a) both two states are the pole states, (b) one is the pole and another one is the continuum states, (c) both two states are the continuum states. In the case (a) we refer as "pole" contribution, which is defined in Ref. [13]. In the cases (b) and (c), we indicate the number of continuum states in the basis set as $N$, and refer as "$SN$."

For the state with angular momenta $l \geq 3$ and $l = 1$; $p_{3/2}$, $p_{1/2}$, $f_{7/2}$, $\cdots$, $h_{9/2}$, no bound nor resonant states are obtained in the region of $\theta = 10$ (degree) of the complex momentum planes. Therefore, the weights of these partial waves automatically become the $S2$-contributions.

We summarize the result for $^{18}$O in Table IV. The main component in $^{18}$O is $(0d_{5/2})^2$, which is the $5/2^+$ ground state of $^{17}$O. Since the $5/2^+$-state is a bound state and has a large binding energy 4.14 (MeV), the $(0d_{5/2})^2$-component becomes dominant in $^{18}$O. The other bound state component, $(1s_{1/2})^2$ is less than 10 percent. Imaginary part of these two bound state contributions comes from a small numerical uncertainty in the expansion of the complex rotated wave function, and those values are very small and less than $10^{-3}$. Therefore, we express these small values as $\epsilon$. The resonant pole contribution becomes complex value. Since the total weight of the wave function is unity, the imaginary part of the $(0d_{3/2})^2$-component compensate to those of the continuum contributions, $S1$ and $S2$.

We show the result of the GSM calculation [14] in the third column of Table IV for a comparison to our COSM.

TABLE IV: Contribution of the poles and continua in $^{18}$O. The core-$n$ eigen states are calculated by CSM with a rotational angle $\theta = 10$ (degree). The Result obtained by GSM is taken from Ref.[14]. In the table, $\epsilon$ are small values, which are less than $10^{-3}$, and each value is not the same.

| $(C_k)^2$ | COSM | GSM [14] |
|---|---|---|
| $(0d_{5/2})^2$ | $0.830 - i\epsilon$ | $0.872 + i\epsilon$ |
| $(1s_{1/2})^2$ | $0.096 - i\epsilon$ | $0.044 - i\epsilon$ |
| $(0d_{3/2})^2$ | $0.028 - i0.005$ | $0.028 - i0.007$ |
| $S1$ | $0.020 + i0.004$ | $0.042 + i0.005$ |
| $S2$ | $0.026 + i0.001$ | $0.015 + i0.002$ |

In the GSM calculation [14], the authors used the surface-delta type $NN$-interaction such as

$$V(r) = -V_0 \, \delta(\boldsymbol{r}_1 - \boldsymbol{r}_2)\delta(r_1 - R_0) \ . \quad (20)$$

This type of interactions has its value only at $r_1 = r_2 = R$. On the other hand, we use the Volkov interaction, which is a finite range Gaussian interaction. Even though the $NN$-interactions for valence nucleons are different between our COSM calculation and the GSM calculation [14], contributions of weights of poles and continua are very similar. We also performed calculations using different types of the $NN$-interaction for the valence neutrons as a check. The contributions of poles and continua are almost the same for several types of the $NN$-interaction. This is because the subsystem $^{17}$O has two bound states, which are well-bound states. Therefore, the dominant part of the ground state of the $^{18}$O eigen function comes from the bound state pole of $^{17}$O, and its contribution is almost independent of the interaction between valence nucleons.

In order to see the isotope dependence of the contributions of the poles and continua, we calculate the contributions of the $0d_{5/2}$-pole and continua of $d_{5/2}$ to the wave functions of oxygen isotopes. Results are shown in Table V. The $0d_{5/2}$-pole contribution is the main part of the wave function and is still dominant in $^{20}$O. Continuum contributions of $d_{5/2}$, $S1$, $S2$, etc., decrease very fast as the number of continuum states increases. The $0d_{5/2}$-pole is the bound state of $^{17}$O. Therefore, a bound state approximation of the wave function or description using only the bound states works very well for the oxygen isotopes.

TABLE V: Contributions of $0d_{5/2}$-pole and continua for the oxygen isotopes

| | $^{18}$O $(0^+)$ | $^{19}$O $(5/2^+)$ | $^{20}$O $(0^+)$ |
|---|---|---|---|
| Poles | 0.830 | 0.868 | 0.782 |
| $S1$ | $3.96 \times 10^{-3}$ | $5.69 \times 10^{-3}$ | $9.45 \times 10^{-3}$ |
| $S2$ | $6.02 \times 10^{-4}$ | $2.37 \times 10^{-4}$ | $3.17 \times 10^{-4}$ |
| $S3$ | —— | $1.53 \times 10^{-5}$ | $2.28 \times 10^{-6}$ |
| $S4$ | —— | —— | $1.55 \times 10^{-7}$ |

### 2. Helium isotopes

For helium isotopes, no bound state exists in the $^4$He+$n$ subsystem. Hence, we construct the extended completeness relation by performing the CSM calculation with a large rotation angle $\theta = 38$ (degree). With this rotation angle, $0p_{3/2}$- and $0p_{1/2}$-pole states are obtained as resonant states with complex eigen values; $0.74 - i0.29$ (MeV) and $2.11 - i2.94$ (MeV), respectively. Although other resonant states with a higher angular momentum are obtained by CSM with the rotation angle $\theta = 38$ (degree), the energy of these resonant states are very high, and the width are large: $0d_{5/2} = 28.5 - i21.6$ (MeV), $0d_{3/2} = 29.1 - i37.3$ (MeV) and $0f_{7/2} = 25.4 - i29.0$ (MeV). Therefore, we do not explicitly treat higher angular momentum states as the pole state and include them in the continua.

Using the extended completeness relation of the $^4$He+$n$ system, we expand the $0^+$ ground state wave function of $^6$He obtained by COSM. Poles and continua contributions are summarized in Table VI. For a comparison, we show GSM results [14, 19] in the third and forth columns of Table VI. Here, we note that the model space and interactions of our COSM calculation and GSM ones are different. In GSM calculations[14, 19], the model space is limited as $l = 1$, i.e. $(p_{3/2})^2$ and $(p_{1/2})^2$, while our COSM calculation is performed with the angular momenta $l \leq 5$, i.e. the highest partial wave is $(h_{11/2})^2$.

TABLE VI: Contribution of the poles and continua for the $^6$He case. The core-$n$ eigen states are calculated by CSM with a rotational angle $\theta = 38$ (degree).

| $(C_k)^2$ | COSM | GSM [14] | GSM [19] |
|---|---|---|---|
| $(0p_{3/2})^2$ | $1.211 - i0.666$ | $0.891 - i0.811$ | $1.105 - i0.832$ |
| $(0p_{1/2})^2$ | $1.447 + i0.007$ | $0.004 - i0.079$ | $0.226 - i0.161$ |
| $S1$ | $-2.909 + i0.650$ | $0.255 + i0.861$ | $-0.259 + i1.106$ |
| $S2$ | $1.251 + i0.009$ | $-0.150 + i0.029$ | $-0.072 - i0.113$ |

As shown in Table VI, the $(0p_{3/2})^2$-pole contribution is the main part. Since the $0p_{3/2}$-state is a resonant state, the contribution becomes a complex values. The imaginary part of the $(0p_{3/2})^2$-pole contribution is large and comparable to that of the real part. Similar to the $^{18}$O case, the $(0p_{3/2})^2$-pole contributions of COSM and GSM are almost the same each other, even though the interaction and model space are different.

TABLE VII: Contribution of the $0p_{3/2}$-pole for helium isotopes.

| | COSM | GSM [14] | GSM [19] |
|---|---|---|---|
| $^6$He | $1.211 - i0.666$ | $0.891 - i0.811$ | $1.105 - i0.832$ |
| $^7$He | $1.429 - i1.017$ | $1.110 - i0.879$ | $1.296 - i0.987$ |
| $^8$He | $0.252 - i1.597$ | $0.296 - i1.323$ | —— |

We calculate isotope dependence of the $(0p_{3/2})^n$-pole contributions in the helium isotopes and show the results in Table VII. Even in $^8$He, our COSM calculation shows the similar behavior to GSM calculations [14, 19] in the real and imaginary parts of the pole contributions.

Next, we consider the pole-continuum correlation in $^6$He. In Table VI, due to the large contribution of the imaginary part of the $(0p_{3/2})^2$-pole, the $S1$ contribution, which has one pole state and one continuum state in the wave function, also has a large imaginary part. This $S1$ contribution is the coefficient of the states which have one pole and one continuum states in the wave function. Therefore, the value indicates the strength of the coupling between the pole and continuum in the view point of the single-particle state.

Contrary to the $0p_{3/2}$ case, the $(0p_{1/2})^2$-pole contribution to the $^6$He ground state obtained by COSM shows a significant difference to that of GSM calculations, see Table VI. The $(0p_{1/2})^2$-pole of our COSM calculation has a large real part, and the absolute value is larger than that of the $(0p_{3/2})^2$-pole. By considering such the large contribution, the $(0p_{1/2})^2$-pole is the important component in $^6$He. Because of the large contribution of the $(0p_{1/2})^2$-pole, the $S1$ contribution of our COSM calculation becomes much larger than those of GSM calculations.

As pointed out in Ref. [25], the "T-base" component, which is one of the rearrangement channel of the coordinate system, is necessary to describe the nucleon-nucleon correlation and is important to reproduce the $^6$He ground state energy. In the "V-base" coordinate system, the component of the T-base coordinate system corresponds to the inclusion of a large number of single-particle states with high angular momenta. In our COSM calculation, we include angular momenta up to $l \leq 5$ into the basis function. This is not sufficient to fully describe the correlation of valence nucleons in the $^6$He ground state, since the convergence of included angular momenta in the basis function to the wave function is very slow and even $l_{max} = 14$ is not enough [25]. However, the large contribution of $(0p_{1/2})^2$-pole in our COSM calculation shows that a part of the important nucleon-nucleon correlation is correctly take into account to the calculation.

In order to make clear the reason of the difference on the $(0p_{1/2})^2$-pole contribution, we perform a calculation with a restricted basis set which only has the angular momentum $l = 1$. In this calculation, only the $p_{3/2}$- and $p_{1/2}$-components are included to the model space. The interaction between valence nucleons is adjusted to reproduce the binding energy of $^6$He, since in this model space, $^6$He cannot be a bound nucleus with the original strength of the interaction. This restricted model space corresponds to that of the GSM calculations [14, 19].

We calculate the pole and continuum contributions. For the continuum contributions, we calculate $p_{3/2}$ and $p_{1/2}$ components separately, and summarize each partial wave as shown in Table VIII. Contributions of $p_{3/2}$; $(0p_{3/2})^2$-pole, $(S1)_{p_{3/2}}$ and $(S2)_{p_{3/2}}$, which are considered to be the main contributions in $^6$He, do not change from the "full"($l \leq 5$) calculation. On the other hand,

contributions of $p_{1/2}$ drastically change from those of the full calculation, and the values become close to those obtained by GSM [19].

Here, we notice that the sum of the $p_{1/2}$ contributions does not change from the full calculation to the restricted one, which are 0.038 and 0.040. Hence, components of higher partial waves in the full calculation are renormalized to the $p_{3/2}$ contributions in the restricted model space calculation, since the sum of $p_{3/2}$ contributions changes from 0.917 to 0.960. For the restricted model space, we adjust the interaction between valence nucleons in order to fit the ground state of $^6$He. This makes the same effect to the transformation of the nucleon-nucleon interaction in Ref. [19].

The contribution of the higher partial waves depends on the model space and the nucleon-nucleon interaction. Microscopic few-body approaches with a finite-range nucleon-nucleon interaction shows the importance of the inclusion the correlation between the valence nucleon. Due to the correlation, the higher partial wave components becomes important in the shell-model-like coordinate systems. In this case, continua of higher waves, which are very important to describe the correlation in the structure of the halo nuclei, are renormalized to the $p_{3/2}$-wave contribution due to the restriction of the model space. As a result, in the restricted model space, the calculated r.m.s.radius of $^6$He becomes much smaller than that of the full calculation. The radius changes from 2.48 (fm) in the full calculation to 2.40 (fm). Hence, if we try to reproduce both the binding energy and r.m.s.radius in the restricted model space, we need to modify interactions between the core and a valence nucleon.

| $(C_k)^2$ | COSM | COSM ($l=1$) | GSM [19] |
|---|---|---|---|
| $(0p_{3/2})^2$ | $1.211 - i0.666$ | $1.139 - i0.742$ | $1.105 - i0.832$ |
| $(\mathrm{S1})_{p_{3/2}}$ | $-0.252 + i0.692$ | $-0.119 + i0.773$ | $-0.060 + i0.881$ |
| $(\mathrm{S2})_{p_{3/2}}$ | $-0.042 - i0.026$ | $-0.060 - i0.031$ | $-0.097 - i0.050$ |
| sum | 0.917 | 0.960 | 0.948 |
| $(0p_{1/2})^2$ | $1.447 + i0.007$ | $0.353 - i0.077$ | $0.226 - i0.161$ |
| $(\mathrm{S1})_{p_{1/2}}$ | $-2.658 - i0.042$ | $-0.534 + i0.065$ | $-0.198 + i0.224$ |
| $(\mathrm{S2})_{p_{1/2}}$ | $1.249 + i0.034$ | $0.221 + i0.012$ | $0.025 - i0.063$ |
| sum | 0.038 | 0.040 | 0.053 |

TABLE VIII: Poles and continua contributions of the $p_{3/2}$- and $p_{1/2}$-components in $^6$He.

We consider the change of these details of the $p_{1/2}$-component shows the importance of the correlation as following reasons. First, oxygen isotopes $^{17-20}$O are normal nuclei not weakly bound systems. In $^{18}$O, even though both the nucleon-nucleon interaction and those model space are different, poles and continuum contributions of $s_{1/2}$-, $d_{5/2}$- and $d_{3/2}$-components are almost the same between COSM and GSM [14]. This is because $^{17}$O has two bound states; $1s_{1/2}$ and $0d_{5/2}$, and these contributions are the main part of the $^{18}$O ground state. Hence, the continuum contributions are not important and the effect of pole-continuum and continuum-continuum couplings become small. Second, different from $^{18}$O, $^6$He is a typical weakly bound and halo nucleus. In the $^4$He+$2n$ model space, there is no bound state in each sub-system, which is called the "Borromean" system. Therefore, components of continuum-continuum coupling and (resonant) pole-continuum coupling become much important. In the "full" ($l \leq 5$) calculation, $(0p_{1/2})^2$-pole, which is a resonant pole, can couple other angular momentum states. When we change the model space to $l = 1$ from the full one, the $(0p_{1/2})^2$-pole has no chance to make a correlation to the higher angular momentum states. Therefore, the $(0p_{1/2})^2$-pole contribution becomes small and is close to that of GSM [19], in which the model space is restricted to $l = 1$.

## IV. SUMMARY AND DISCUSSION

We studied pole and continuum contributions to the wave function obtained by COSM. As examples of normal nuclei and weakly bound nuclei, we study oxygen and helium isotopes. Binding energies and r.m.s.radii of the oxygen and helium isotopes calculated by COSM reasonably agrees with the experimental ones. Therefore, the wave function reproduces the ground state properties of these isotopes at least in the view point of the core+$Xn$ model space.

In our COSM formalism, the wave function is constructed by a linear combination of Gaussian with different width parameters, which are non-orthogonal basis sets. Width parameters and angular momenta in the basis sets are chosen by a stochastic approach. Hence, in order to investigate the contributions of poles and continua of the single-particle states, we expand the wave function obtained by COSM. To prepare the completeness relation of the single-particle states, we solve the complex scaled Hamiltonian of the core+$N$ system using CSM.

We found the correspondence to GSM in the oxygen isotopes, and the significant difference in $(0p_{1/2})^2$-pole contribution in $^6$He. We consider this difference is important to make clear a key point of the COSM formalism. Because, even though basis sets are truncated due to the finite basis size, COSM can take into account important correlations of valence nucleons at a maximum.

There still remains a open question whether the asymptotic condition of the single-particle unbound states can satisfy that of a many-particle bound state. In the COSM approach with the Gaussian basis sets, bound state asymptotic condition is satisfied, since the basis set already satisfy the condition. On the other hand, GSM approach constructs the wave function of a many-body bound state from the single-particle complete set, which include continuum states.

Further, the treatment of the non-central force in the $NN$-interaction and the effect of the core-polarization is important and will be the future work.

**Acknowledgments**

The authors would like to thank the members of the nuclear theory group in Hokkaido University for their kind interest and discussions. The authors also thank Prof. Motobayashi and Dr. Myo for the fruitful discussion. This work is partially performed in the Research Project for Study of Unstable Nuclei from Nuclear Cluster Aspects sponsored by Institute of Physical and Chemical Research (RIKEN).

[1] A. Ozawa *et al.*, Nucl. Phys. **A691**, 599 (2001).
[2] A. Ozawa, T. Suzuki, and I. Tanihata, Nucl. Phys. **A693**, 32 (2001).
[3] R. Kanungo *et al.*, Phys. Rev. Lett. **88**, 142502 (2002).
[4] R. Kanungo, I. Tanihata, and A. Ozawa, Phys. Lett. **B512**, 261 (2001).
[5] O. Tarasov *et al.*, Phys. Lett. **B409**, 64 (1997).
[6] H. Sakurai *et al.*, Phys. Lett. **B448**, 180 (1999).
[7] H. Y. Zhang *et al.*, Nucl. Phys. **A707**, 303 (2002).
[8] E. Khan *et al.*, Phys. Lett. **B490**, 45 (2000).
[9] U. Fano, Phys. Rev. **124**, 1866 (1961).
[10] C. Mahaux and H. Weidenmüller, *Shell Model Approaches to Nuclear Reactions*, North-Holand, Amsteldom, 1969.
[11] J. Okołowicz, M. Płoszajczak and I. Rotter, Phys. Rep. **374**, 271 (2003).
[12] K. Bennaceur, F. Nowacki, J. Okołowicz and M. Płoszajczak, Nucl. Phys. **A671**, 203 (2000).
[13] N. Michel, W. Nazarewicz, M. Płoszajczak and K. Bennaceur, Phys. Rev. Lett. **89**, 042502 (2002).
[14] N. Michel, W. Nazarewicz, M. Płoszajczak and J. Okołowicz, Phys. Rev. C **67**, 054311 (2003).
[15] N. Michel, W. Nazarewicz and M. Płoszajczak, Phys. Rev. C **70**, 064313 (2004).
[16] R. Id Betan, R. J. Liotta, N. Sandulescu and T. Vertse, Phys. Rev. Lett. **89**, 042501 (2002).
[17] R. Id Betan, R. J. Liotta, N. Sandulescu and T. Vertse, Phys. Rev. C **67**, 014322 (2003).
[18] R. Id Betan, R. J. Liotta, N. Sandulescu and T. Vertse, Phys. Lett. **B584**, 48 (2004).
[19] G. Hagen, M. Hjorth-Jensen and J. S. Vaagen, Phys. Rev. C **71**, 044314 (2005).
[20] T. Berggren, Nucl. Phys. **A109**, 265 (1968).
[21] T. Berggren and P. Lind, Phys. Rev. C **47**, 768 (1992).
[22] G. Gamow, Z. Phys. **51**, 204 (1928); **52**, 510 (1928).
[23] I. Tanihata *et al.*, Phys. Rev. Lett. **55**, 2676 (1985).
[24] Y. Tosaka, Y. Suzuki, and K. Ikeda, Prog. Theor. Phys. **88**, 1140 ( 1990).
[25] S. Aoyama, S. Mukai, K. Katō and K. Ikeda, Prog. Theor. Phys. **93**, 99 (1995).
[26] T. Myo, S. Aoyama, K. Katō and K. Ikeda, Prog. Theor. Phys. **108**, 133 (2002).
[27] T. Myo, K. Katō, S. Aoyama and K. Ikeda, Phys. Rev. C **63**, 054313 (2001).
[28] S. Aoyama, T. Myo, K. Katō and K. Ikeda, Prog. Theor. Phys. **116**, 1 (2006).
[29] H. Masui, K. Katō, and K. Ikeda, Phys. Rev. **C73**, 034318 (2006).
[30] Y. Suzuki and K. Ikeda, Phys. Rev. C **38**, 410 (1988).
[31] J. Aguilar and J. M. Combes, Commun. Math. Phys. **22**, 269 (1971).
[32] E. Balslev and J. M. Combes, Commun. Math. Phys. **22**, 280 (1971).
[33] Y.K. Ho, Phys. Rept. **99**, 1 (1983).
[34] T. Myo, A. Ohnishi, and K. Katō, Prog. Theor. Phys. **99**, 801 (1998).
[35] T. Kaneko, M. LeMere and Y. C. Tang, Phys. Rev. C **44**, 1588 (1991).
[36] S. Saito, Prog. Theor. Phys. Suppl. **62**, 11 (1977).
[37] A. B. Volkov, Nucl. Phys. **74**, 33 (1965).
[38] F. Ajzenberg-Selove, Nucl. Phys. **A460**, 1 (1986).
[39] F. Ajzenberg-Selove, Nucl. Phys. **A475**, 1 (1987).
[40] H. Kanada, T. Kaneko, S. Nagata, and M. Nomoto, Prog. Theor. Phys. **61**, 1327 (1979).
[41] D. R. Thompson, M. LeMere, and Y. C. Tang, Nucl. Phys. **A286**, 53 (1977).
[42] F. Ajzenberg-Selove, Nucl. Phys. **A490**, 1 (1988).
[43] I. Tanihata, Nucl. Phys. **A478**, 795c (1998)
[44] I. Tanihata *et al.*, Phys. Lett. B **289**, 261 (1992).
[45] G. D. Alkhazov *et al.*, Phys. Rev. Lett. **78**, 2313 (1997).